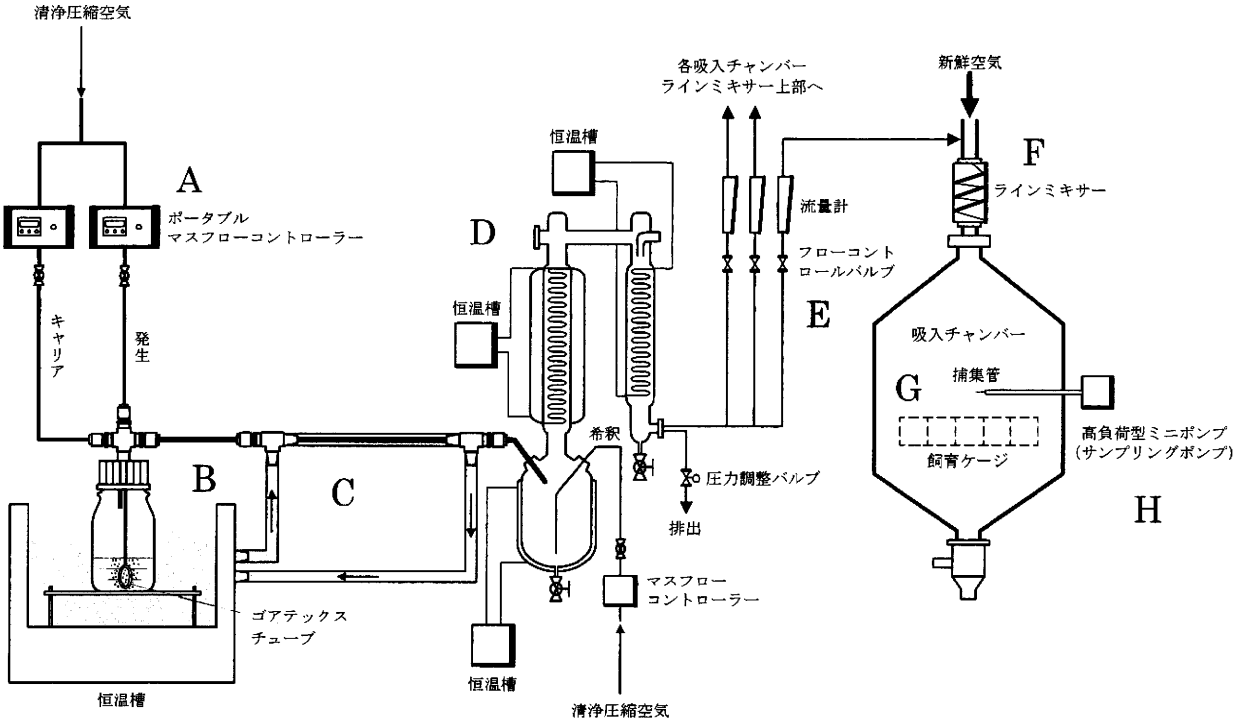

図 ダイアジノン-1　吸入暴露装置のシステム

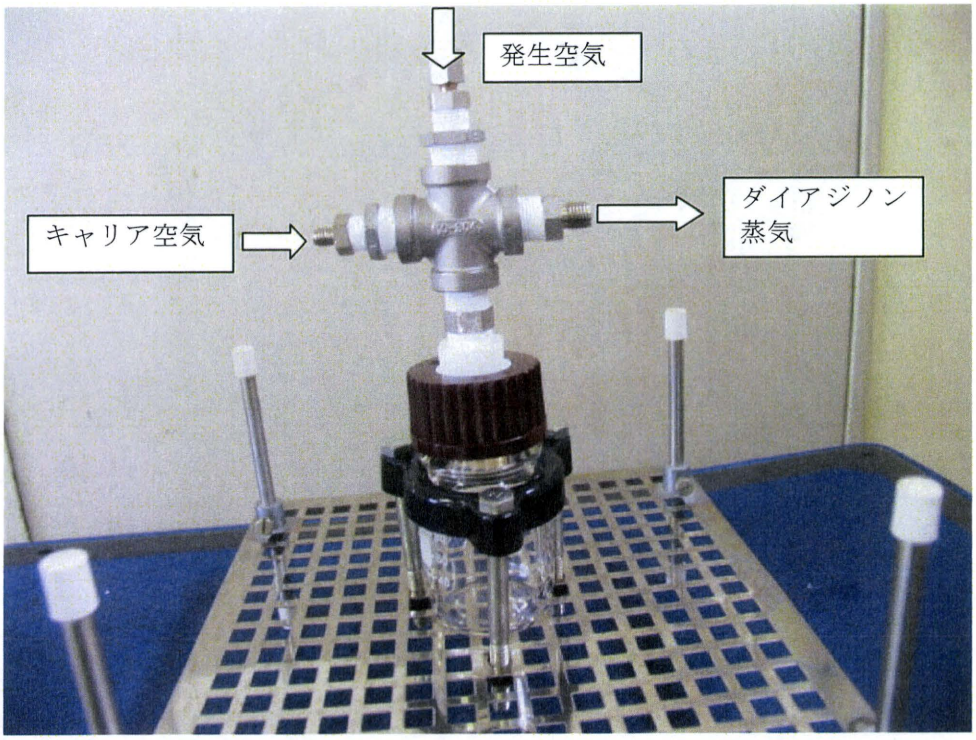

図 ダイアジノン-2　ダイアジノンの発生容器

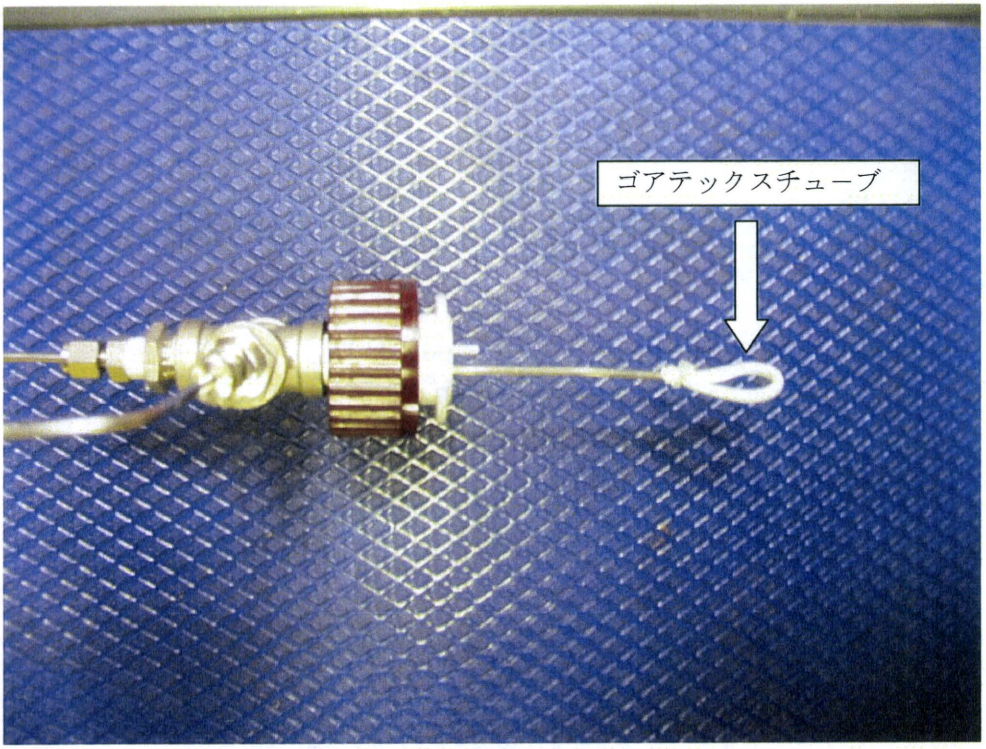

図 ダイアジノン-3　ゴアテックスチューブ（矢印）を装着したバブリング部分

図 ダイアジノン-4　ゴアテックスチューブによるダイアジノンの気泡の発生状態

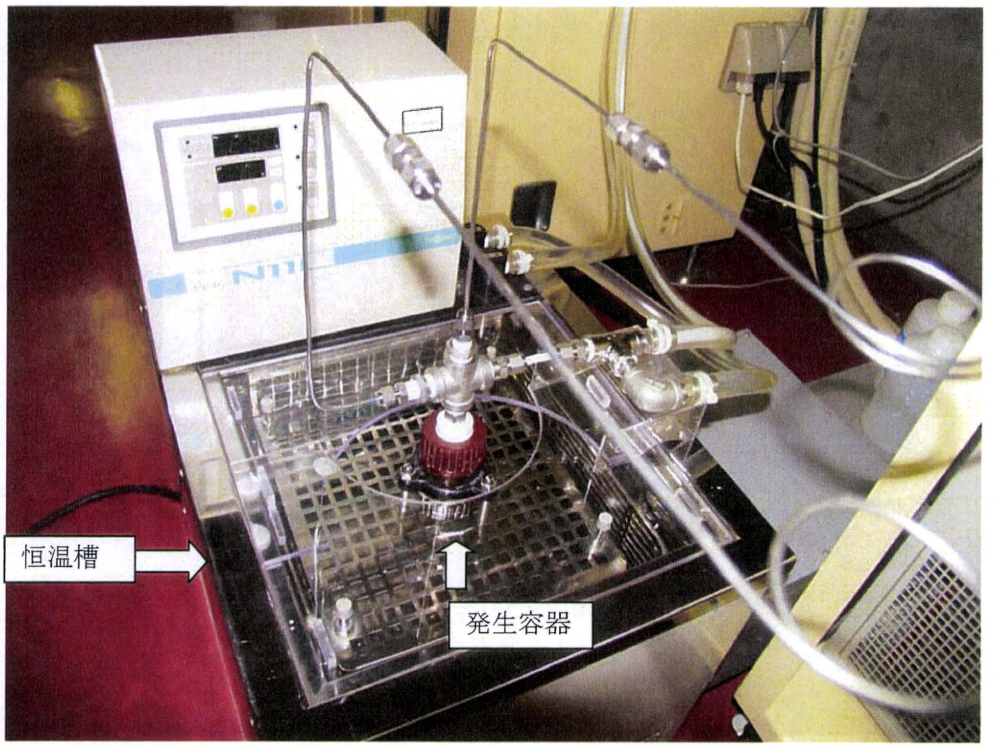

図 ダイアジノン-5　恒温槽内に設置したダイアジノンの発生容器

別添 4

Ⅱ．研究成果の刊行に関する一覧表

発表者氏名	論文タイトル名	発表誌名	巻名	ページ	出版年
Xu J, Futakuchi M, Iigo M, Fukamachi K, Alexander DB, Shimizu H, Sakai Y, Tamano S, Furukawa F, Uchino T, Tokunaga H, Nishimura T, Hirose A, Kanno J, Tsuda H.	Involvement of macrophage inflammation protein 1α (MIP1α) in promotion of rat lung and mammary carcinogenic activity of nano-scale titanium dioxide particles administered by intra-pulmonary spraying.	Carcinogenesis	31 (5)	927 - 935	2010
Take, M., Yamamoto, S., Ohnishi, M., Matsumoto, M., Nagano, K., Hirota, T., Fukushima, S	Chloroform distribution and accumulation by combined inhalation plus oral exposure routes in rats.	J of Environmental Science and Health Part A	45	1616 - 1624	2010
Umeda, Y., Matsumoto, M., Aiso, S., Nishizawa, T, Nagano, K., Arito, H. and Fukushima S.	Inhalation carcinogenicity and toxicity of 1,2-dichloropropane in rats.	Inhalation Toxicology	22	1116 - 1126	2010
Renne, R., Brix, A., Harkema, J., Herbert, R., Kittel, B., Lewis, D., March, T., Nagano, K., Pino, M., Rittinghausen, S., Rosenbruch, M., Tellier, P., Wohrmann, T.	Proliferative and nonproliferative lesions of the rat and mouse respiratory tract	Toxicologic Pathology	37	5S - 73S	2009
Uchida K, Nakata K, Suzuki T, Luisetti M, Watanabe M, Koch DE, Stevens CA, Beck DC, Denson LA, Carey B, Keicho N, Krischer JP, Yamada Y, Trapnell BC.	Granulocyte/Macrophage Colony-Stimulating Factor Autoantibodies and Myeloid Cell Immune Functions in Healthy Individuals.	Blood	113	2547 - 2556	2009
Kawasaki, Y., Hirabayashi, Y., Kaneko, T., Kanno, J., Kodama, Y., Matsushima, Y., Ogawa, Y., Saitoh, M., Uchida, O., Umemura, T., Yoon, B., Inoue, T.	Benzen-Induced Hematopoietic Neoplasms Including Myeloid Leukemia in Trp53-Deficient C57BL/6 andC3H/He Mice.	Toxicol. Science	110 (2)	293 - 306	2009

Hang NTL, Ishizuka N, Keicho N, Hong LT, Tam DB, Thu VTX, Matsushita I, Harada N, Higuchi K, Sakurada S, Lien LT.	Quality assessment of an interferon-gamma release assay for tuberculosis infection in a resource-limited setting.	BMC Infect Dis	9:66		2009
Kanno J.	Overview: "Children's toxicology", a renovating study field of irreversible "early exposure-delayed effects".	J Toxicol Sci.	34 Suppl 2	SP 199 - 200	2009
Tanemura K, Igarashi K, Matsugami TR, Aisaki K, Kitajima S, Kanno J.	Intrauterine environment-genome interaction and children's development (2): Brain structure impairment and behavioral disturbance induced in male mice offspring by a single intraperitoneal administration of domoic acid (DA) to their dams.	J Toxicol Sci.	34 Suppl 2	SP 279 - 286	2009
Ohbayashi, H., Umeda, Y., Senoh, H., Kasai, Kano, H., Nagano, K., Arito, H. and Fukushima, S.	Enhanced hepatocarcinogenicity by combined inhalation and oral exposures to N,N-dimethylformamide in male rats	J Toxicol. Sci.	34	53 - 63	2009
Takagi A, Hirose A, Nishimura T, Fukumori N, Ogata A, Ohashi N, Kitajima S, Kanno J.	Induction of mesothelioma in p53+/- mouse by intraperitoneal application of multi-wall carbon nanotube.	J Toxicol Sci.	33	105 - 116	2008
Kasai, T., Saito, M., Senoh, H., Umeda, Y., Aiso, S., Ohbayashi, H, Nishizawa, T., Nagano, K. and Fukushima, S.	Thirteen-week inhalation toxicity of 1,4-dioxane in rats	Inhalation Toxicology	20	961 - 971	2008

Ⅲ. 研究成果の刊行物・別刷

Carcinogenesis vol.31 no.5 pp.927–935, 2010
doi:10.1093/carcin/bgq029
Advance Access publication February 25, 2010

Involvement of macrophage inflammatory protein 1α (MIP1α) in promotion of rat lung and mammary carcinogenic activity of nanoscale titanium dioxide particles administered by intra-pulmonary spraying

Jiegou Xu[1], Mitsuru Futakuchi[1], Masaaki Iigo[1], Katsumi Fukamachi[1], David B.Alexander[1], Hideo Shimizu[2], Yuto Sakai[1,3], Seiko Tamano[4], Fumio Furukawa[4], Tadashi Uchino[5], Hiroshi Tokunaga[6], Tetsuji Nishimura[5], Akihiko Hirose[5], Jun Kanno[5] and Hiroyuki Tsuda[1,*]

[1]Department of Molecular Toxicology and [2]Core Laboratory, Nagoya City University Graduate School of Medical Sciences, 1-Kawasumi, Mizuho-cho, Mizuho-ku, Nagoya 467-8601, Japan, [3]Department of Drug Metabolism and Disposition, Graduate School of Pharmaceutical Sciences, 3-1, Tanabe-Dohri, Mizuho-ku, Nagoya 467-8603, Japan, [4]DIMS Institute of Medical Science, Inc., 64 Goura, Nishiazai, Azai-cho, Ichinomiya 491-0113, Japan, [5]National Institute of Health Sciences, 1-18-1 Kamiyoga, Setagaya-ku, Tokyo 158-8501, Japan and [6]Pharmaceuticals and Medical Devices Agency, 2-3-3, Kasumigaseki, Chiyoda-ku, Tokyo 100-0013, Japan

*To whom correspondence should be addressed. Tel: +81 52 853 8991; Fax: +81 52 853 8996;
Email: htsuda@med.nagoya-cu.ac.jp

Titanium dioxide (TiO_2) is evaluated by World Health Organization/International Agency for Research on Cancer as a Group 2B carcinogen. The present study was conducted to detect carcinogenic activity of nanoscale TiO_2 administered by a novel intrapulmonary spraying (IPS)-initiation–promotion protocol in the rat lung. Female human c-Ha-*ras* proto-oncogene transgenic rat (H*ras*128) transgenic rats were treated first with *N*-nitrosobis(2-hydroxypropyl)amine (DHPN) in the drinking water and then with TiO_2 (rutile type, mean diameter 20 nm, without coating) by IPS. TiO_2 treatment significantly increased the multiplicity of DHPN-induced alveolar cell hyperplasias and adenomas in the lung, and the multiplicity of mammary adenocarcinomas, confirming the effectiveness of the IPS-initiation–promotion protocol. TiO_2 aggregates were localized exclusively in alveolar macrophages and had a mean diameter of 107.4 nm. To investigate the underlying mechanism of its carcinogenic effects, TiO_2 was administered to wild-type rats by IPS five times over 9 days. TiO_2 treatment significantly increased 8-hydroxydeoxy guanosine level, superoxide dismutase activity and macrophage inflammatory protein 1α (MIP1α) expression in the lung. MIP1α, detected in the cytoplasm of TiO_2-laden alveolar macrophages *in vivo* and in the media of rat primary alveolar macrophages treated with TiO_2 *in vitro*, enhanced proliferation of human lung cancer cells. Furthermore, MIP1α, also detected in the sera and mammary adenocarcinomas of TiO_2-treated H*ras*128 rats, enhanced proliferation of rat mammary carcinoma cells. These data indicate that secreted MIP1α from TiO_2-laden alveolar macrophages can cause cell proliferation in the alveoli and mammary gland and suggest that TiO_2 tumor promotion is mediated by MIP1α acting locally in the alveoli and distantly in the mammary gland after transport via the circulation.

Introduction

Inhalation of particles and fiber is well known to be strongly associated with increased lung cancer risk in the workplace (1,2). Although the size of fiber particles was reported to be closely related to risk (3), the precise role of particles and fibers in lung cancer induction has not yet been elucidated.

Titanium dioxide (TiO_2) particles of various sizes are manufactured worldwide in large quantities and are used in a wide range of applications. TiO_2 particles have long been considered to pose little risk to respiratory health because they are chemically and thermally stable. However, TiO_2 is classified as a Group 2B carcinogen, a possible carcinogen to humans, by World Health Organization/International Agency for Research on Cancer based on the findings of lung tumor induction in female rats (3,4). This overall evaluation includes nanoscale (<100 nm in diameter) and larger sized classes of TiO_2. At present, the mechanism underlying the development of rat lung tumors by inhalation of TiO_2 particles is unclear.

Inhalation of TiO_2 particles can occur both at the workplace, e.g. in manufacturing and packing sites, and also outside the workplace during their use (5–7). Exposure to airborne nanoparticles has been reported to be associated with a granulomatous inflammatory response in the lung (8). Inhalation studies of nanoparticles for cancer risk assessment is urgently needed, however, due to the high cost of long-term studies, available data is severely limited (9,10). The aim of this study is to understand the mechanism underlying rat lung carcinogenesis induced by inhalation of TiO_2 particles. We choose intrapulmonary spraying (IPS) because it does not require costly facilities, allows accurate dose control and approximates long-term inhalation studies (3,11).

We initially examined whether TiO_2 particles have carcinogenic activity in the rat lung using a novel IPS-initiation–promotion protocol (12,13). For these experiments, Sprague–Dawley (SD)-derived female human c-Ha-*ras* proto-oncogene transgenic rat (H*ras*128) transgenic rats, which are known to have the same carcinogen susceptibility phenotype in the lung as wild-type rats but are highly susceptible to mammary tumor induction (14–16), were treated with *N*-nitrosobis(2-hydroxypropyl)amine (DHPN) to initiate carcinogenesis and then treated with TiO_2 by IPS. We observed a promotion effect of TiO_2 particles in lung and mammary gland carcinogenesis.

To identify factors involved in this promotion effect, wild-type SD strain rats were treated with TiO_2 by IPS for 9 days. We found macrophage inflammatory protein 1α (MIP1α) was produced by TiO_2-laden alveolar macrophages in the lungs of rats treated with TiO_2. MIP1α is a member of the CC chemokine family and is primarily associated with cell adhesion and migration of multiple myeloma cells (17). It is reported to be produced by macrophages in response to a variety of inflammatory stimuli including TiO_2 (18). In the present study, MIP1α, detected in the medium of rat primary alveolar macrophages treated with TiO_2, enhanced proliferation of human lung cancer cells *in vitro*. MIP1α was also detected in the sera and mammary adenocarcinomas of TiO_2-treated H*ras*128 rats and enhanced proliferation of rat mammary carcinoma cells.

Materials and methods

Animals

Female transgenic rats carrying the H*ras*128 and female wild-type SD rats were obtained from CLEA Japan Co., Ltd (Tokyo, Japan) (15). The animals were housed in the animal center of Nagoya City University Medical School, maintained on a 12 h light–dark cycle and received Oriental MF basal diet (Oriental Yeast Co., Tokyo, Japan) and water *ad libitum*. The research was conducted according to the Guidelines for the Care and Use of Laboratory Animals of

Abbreviations: CCR1, C-C chemokine receptor type 1; DHPN, *N*-nitrosobis (2-hydroxypropyl) amine; ERK, extracellular signal-regulated kinase; GRO, growth-regulated oncogene; H*ras*128 rat, human c-Ha-*ras* proto-oncogene transgenic rat; IL, interleukin; IPS, intrapulmonary spraying; MEK1, MAPK/ERK kinase1; MIP1α, macrophage inflammatory protein 1α; 8-OHdG, 8-hydroxydeoxy guanosine; PBS, phosphate-buffered saline; ROS, reactive oxygen species; SD, Sprague–Dawley; SOD, superoxide dismutase; TEM, transmission electron microscopy; TiO_2, titanium dioxide.

Nagoya City University Medical School and the experimental protocol was approved by the Institutional Animal Care and Use Committee (H17-28).

Preparation of TiO_2 and IPS

TiO_2 particles (rutile type, without coating; with a mean primary size of 20 nm) were provided by Japan Cosmetic Association, Tokyo, Japan. TiO_2 particles were suspended in saline at 250 μg/ml or 500 μg/ml. The suspension was autoclaved and then sonicated for 20 min just before use. The TiO_2 suspension was intratracheally administered to animals under isoflurane anesthesia using a Microsprayer (Series IA-1B Intratracheal Aerosolizer, Penn-Century, Philadelphia, PA) connected to a 1 ml syringe; the nozzle of the sprayer was inserted into the trachea through the larynx and a total of 0.5 ml suspension was sprayed into the lungs synchronizing with spontaneous respiratory inhalation (IPS).

IPS-initiation–promotion protocol

Thirty-three female H*ras*128 rats aged 6 weeks were given 0.2% DHPN, (Wako Chemicals Co., Ltd Osaka, Japan) in the drinking water for 2 weeks and 9 rats were given drinking water without DHPN. Two weeks later, the rats were divided into four groups, DHPN alone (Group 1), DHPN followed by 250 μg/ml TiO_2 (Group 2), DHPN followed by 500 μg/ml TiO_2 (Group 3) and 500 μg/ml TiO_2 without DHPN (Group 4). The TiO_2 particle preparations were administered by IPS once every 2 weeks from the end of week 4 to week 16 (a total of seven times). The total amount of TiO_2 administered to Groups 1, 2, 3 and 4 were 0, 0.875, 1.75 and 1.75 mg per rat, respectively. Three days after the last treatment, animals were killed and the organs (brain, lung, liver, spleen, kidney, mammary gland, ovaries, uterus and neck lymph nodes) were excised and divided into two pieces; one piece was immediately frozen at −80°C and used for quantitative measurement of elemental titanium, and the other piece was fixed in 4% paraformaldehyde solution in phosphate-buffered saline (PBS) buffer adjusted to pH 7.3 and processed for light microscopic examination and transmission electron microscopy (TEM); the left lungs and inguinal mammary glands were used for elemental titanium analysis and the right lungs and inguinal mammary glands were used for microscopic examination.

IPS 9 day protocol

Twenty female SD rats (wild-type counterpart of H*ras*128) aged 10 weeks were treated by IPS with 0.5 ml suspension of 500 μg/ml TiO_2 particles in saline five times over a 9 day period (Figure 2A). The total amount of TiO_2 administered was 1.25 mg per rat. Six hours after the last dose, animals were killed and the lungs and inguinal mammary glands were excised. Fatty tissue surrounding the mammary gland was removed as much as possible. The left lungs and inguinal mammary glands were used for biochemical analysis, and the right lungs were fixed in 4% paraformaldehyde solution in PBS adjusted at pH 7.3 and processed for histopathological examination and immunohistochemistry.

Light microscopic and TEM observation of TiO_2 particles in the lung

Paraffin blocks were deparaffinized and embedded in epon resin and processed for TiO_2 particle observation and titanium element analysis, using a JEM-1010 transmission electron microscope (JEOL Co. Ltd, Tokyo, Japan) equipped with an X-ray microanalyzer (EDAX, Tokyo, Japan). Size analysis of TiO_2 particles was performed using TEM photos by an image analyzer system, (IPAP, Sumika Technos Corporation, Osaka, Japan). A total of 452 particles from alveolar macrophages from rats in Group 3 (DHPN followed by 500 μg/ml TiO_2) of the IPS-initiation–promotion study and a total of 2571 particles from alveolar macrophages from rats in the IPS 9 day study were measured.

Biochemical element analysis of titanium

For the detection of elemental titanium, frozen tissue samples of 50–100 mg were digested with 5 ml concentrated HNO_3 for 22 min in a microwave oven. Titanium in the digested solutions was determined by inductively coupled plasma–mass spectrometry (HP-4500, Hewlett-Packard Co., Houston, TX) under the following conditions: RF power, 1450 W; RF refraction current, 5 W; Plasma gas current, 15 l/min; Carrier gas current, 0.91 l/min; Peri pump, 0.2 r.p.s.; Monitoring mass-m/z 48 (Ti); Integrating interval, 0.1 s; Sampling period 0.31 s.

Analysis of superoxide dismutase activity, 8-hydroxydeoxy guanosine and cytokine levels

For the analysis of superoxide dismutase (SOD) activity, 8-hydroxydeoxy guanosine (8-OHdG) and cytokine levels, animals exposed to TiO_2 particles for 9 days were used. For 8-OHdG levels, genomic DNA was isolated from the left lung and inguinal mammary gland with a DNA Extractor WB Kit (Wako Chemicals Co. Ltd). 8-OHdG levels were determined with an 8-OHdG ELISA Check Kit (Japan Institute for the Control of Aging, Shizuoka, Japan) and by a custom service (OHG Institute Co., Ltd, Fukuoka, Japan). For the analysis of SOD activity and inflammation-related cytokines, tissue from the left lung and inguinal mammary glands was excised and rinsed with cold PBS three times and homogenized in 1 ml of T-PER, Tissue Protein Extraction Reagent (Pierce, Rockford, IL), containing 1% (vol/vol) proteinase inhibitor cocktail (Sigma–Aldrich, St Louis, MO). The homogenates were clarified by centrifugation at 10 000*g* for 5 min at 4°C. Protein content was measured using a BCA™ Protein Assay Kit (Pierce). SOD activity was determined using an SOD Assay Kit (Cayman Chemical Co., Ann Arbor, MI). The levels of interleukin (IL)-1α, IL-1β, IL-6, granulocyte-macrophage colony-stimulating factor, granulocyte colony-stimulating factor, tumor necrosis factor α, interferon γ, IL-18, monocyte chemotactic protein 1 and MIP1α, growth-regulated oncogene (GRO) and vascular endothelial growth factor were measured by Multiplex Suspension array (GeneticLab Co., Ltd, Sapporo, Japan).

Immunohistochemistry

CD68 and MIP1α were detected using anti-rat CD68 (BMA Biomedicals, Augst, Switzerland) and anti-rat MIP1α polyclonal antibodies (BioVision, Lyon, France). Both antibodies were diluted 1:100 in blocking solution and applied to slides, and the slides were incubated at 4°C overnight. The slides were then incubated for 1 h with biotinylated species-specific secondary antibodies diluted 1:500 (Vector Laboratories, Burlingame, CA) and visualized using avidin-conjugated alkaline phosphatase complex (ABC kit, Vector Laboratories) and Alkaline Phosphatase Substrate Kit (Vector Laboratories).

Isolation of primary alveolar macrophages and preparation of conditioned media

Wild-type female SD rats were given 0.5 ml 6% thioglycollate medium (Thioglycollate Medium II, Eiken Chemical Co., Ltd, Tokyo, Japan) by IPS on days 1, 3 and 5, and 6 h after the last treatment, the lungs were excised and minced with sterilized scissors in RPMI 1640 containing 10% fetal bovine serum (Wako Chemicals Co., Ltd) and antibiotics. The homogenate was washed twice and plated onto 6 cm dishes and incubated for 2 h at 37°C, 5% CO_2. The dishes were then washed with PBS three times to remove unattached cells and cell debris. Samples of the remaining adherent cells were cultured in chamber slides and immunostained for CD68 to confirm their identity as macrophages; ~98% of the cells were positive for CD68.

Primary alveolar macrophages were treated with vehicle or TiO_2 particles in saline suspension at a final concentration of 100 μg/ml and then incubated for 24 h in a 37°C, 5% CO_2 incubator. The conditioned medium was collected and diluted 5-fold with RPMI 1640; the conditioned medium had a final concentration of 2% fetal bovine serum.

Western blotting

For the detection of MIP1α, aliquots of 20 μg protein from the extracts of lung or mammary tissue were separated by 15% sodium dodecyl sulfate–polyacrylamide gel electrophoresis, transferred to nitrocellulose membranes and immunoblotted. For the detection of C-C chemokine receptor type 1 (CCR1), 10% sodium dodecyl sulfate–polyacrylamide gel electrophoresis was used for the separation. Membranes were probed overnight at 4°C with anti-rat MIP1α polyclonal antibody (BioVision) diluted at 1:100 or anti-CCR1 (Santa Cruz Biotechnology, Santa Cruz, CA) diluted at 1:100. The blots were washed and incubated for 1 h with biotinylated anti-species-specific secondary antibodies (Amersham Biosciences, Piscataway, NJ) and then visualized using ECL Western Blotting Detection Reagent (Amersham Biosciences). To ensure equal protein loading, the blots were striped with Restore Western Blot Stripping Buffer (Pierce) and reprobed with anti-β actin antibody (dilution 1:2000; Sigma–Aldrich) for 1 h at room temperature.

For the detection of serum MIP1α, GRO and IL-6, aliquots of 150 μg of protein from the sera of rats treated with TiO_2 for 16 weeks were subjected to sodium dodecyl sulfate–polyacrylamide gel electrophoresis. Anti-human GRO polyclonal antibody (BioVision) and anti-mouse IL-6 polyclonal antibody (Santa Cruz) were diluted 1:100. For detection of activated extracellular signal-regulated kinase (ERK) 1/2 and total ERK1/2, phospho ERK1/2 antiboby (Cell signaling Technology, Beverly, MA) and ERK1/2 antibody (Upstate, Lake placid, NY) were diluted 1:2000 and 1:25 000, respectively. The conditioned medium from alveolar macrophages, prepared as described above, was also subjected to western blot assay for MIP1α detection as described above. The blots were striped with Restore Western Blot Stripping Buffer (Pierce) and stained with Ponceau S solution (Sigma–Aldrich) for 10 min. The major band at 66 kDa was judged to be albumin and used as an internal control.

In vitro cell proliferation assay

A549 cells, a human lung cancer cell line, and the rat mammary cancer cell line C3 (19), derived from the H*ras*128 transgenic rats, were used in the *in vitro* cell proliferation assays. A549 or C3 cells were seeded into 96-well culture plates at 5×10^3 cells per well in 2% fetal bovine serum Dulbecco's modified Eagle's medium (Wako Chemicals Co., Ltd). After overnight incubation, the cells were treated as noted below, incubated for 72 h and the relative cell number was then determined.

To investigate the effect of culture supernatant from alveolar macrophages on A549 cell proliferation, their media were replaced with diluted conditioned medium, and the cells were incubated for 72 h with 0, 5, 10 and 20 μg/ml of anti-MIP1α neutralizing antibody (R&D Systems, Minneapolis, MN) or with 20 μg/ml of irrelevant IgG. To investigate the effect of recombinant cytokines on A549 cell proliferation, 10, 50 or 100 ng/ml of recombinant protein, rat MIP1α (R&D Systems), human GRO (R&D Systems) or human IL-6 (R&D Systems), was added to A549 cells. To investigate the role of ERK in MIP1α-stimulated cell proliferation, A549 cells, treated with or without 2×10^{-7} M of the specific MAPK/ERK kinase1 (MEK1) inhibitor PD98059 (Cell Signaling Technology) for 10 min, were treated with 50 ng/ml of MIP1α protein. To investigate the effect of reactive oxygen species (ROS) on cell proliferation, A549 cells, with or without pretreatment with 1 mM *N*-acetyl cysteine (Wako Chemicals Co. Ltd) for 30 min, were treated with 0.5 mM H_2O_2 (Wako Chemicals Co. Ltd). To investigate of the effects of MIP1α on rat mammary cells, C3 cells were treated with serially diluted recombinant rat MIP1α (0, 0.4, 2.0, 10 and 50 ng/ml, respectively; R&D Systems). For detecting the direct effect of TiO_2 particles on A549 and C3 cell proliferation, 5×10^3 A549 or C3 cells were cultured overnight and then treated with 10 or 50 μg/ml of TiO_2 particles.

After 72 h incubation, the relative cell number of A549 and C3 was determined using the Cell Counting Kit-8 (Dojindo Molecular Technologies, Rockville, MD) according to the manufacturer's instruction.

Statistical analysis

For *in vivo* data, statistical analysis was performed using the Kruskal–Wallis and Bonferroni–Dunn's multiple comparison tests. *In vitro* data are presented as means ± standard deviations. The statistical significance of *in vitro* findings was analyzed using a two-tailed Student's *t*-test and Bonferroni–Dunn's multiple comparison tests. A value of $P < 0.05$ was considered significant. The Spearman's rank correlation test was used to determine the association between TiO_2 dose and TiO_2 carcinogenic activity.

Results

Promoting effects of TiO_2 particles in DHPN-induced lung and mammary carcinogenesis

Prior to initiation of the IPS-initiation–promotion and IPS 9 day studies, we conducted a preliminary study to confirm whether IPS would be a good tool to deliver TiO_2 particles to the alveoli. Rats were treated by IPS with India ink. We observed that ink particles of ~50 to 500 μm in diameter were diffusely distributed throughout the alveoli space (data not shown), confirming that IPS could deliver TiO_2 particles to the alveoli.

Four groups of female H*ras*128 rats were treated with +/− DHPN to initiate carcinogenesis and then treated with TiO_2 by IPS for 12 weeks: Group 1, DHPN alone; Group 2, DHPN followed by 250 μg/ml TiO_2; Group 3, DHPN followed by 500 μg/ml TiO_2 and Group 4, 500 μg/ml TiO_2 without DHPN. Microscopic observation in the lung showed scattered inflammatory foci, alveolar cell hyperplasia (Figure 1A) and adenomas in the DHPN-treated rats. The multiplicity (numbers per square centimeter lung) of hyperplasias and adenomas in Group 3 (DHPN followed by 500 μg/ml TiO_2) were significantly increased compared with Group 1 (DHPN followed by saline, Table I), and the increase showed a dose-dependent correlation (rho = 0.630, $P = 0.001$ for hyperplasias and rho = 0.592, $P = 0.029$ for adenomas) by the Spearman's rank correlation test. In the mammary gland, TiO_2 treatment significantly increased the multiplicity of adenocarcinomas (Figure 1C) and tended to increase the weight of the mammary tumors (Figure 1C). In the rats, which received TiO_2 treatment without prior DHPN treatment, alveolar proliferative lesions were not observed although slight inflammatory lesions were observed.

TiO_2 was distributed primarily to the lung, but minor amounts of TiO_2 were also found in other organs (supplementary Figure 1A is available at *Carcinogenesis* Online).

Various sizes of TiO_2 aggregates were observed in alveolar macrophages (Figure 1B). The TiO_2-laden macrophages were evenly scattered throughout the lung alveoli. The number of hyperplasias with TiO_2-laden macrophages was dose dependently increased (supplementary Table 1 is available at *Carcinogenesis* Online). This result suggests that TiO_2-laden macrophages may be involved in the promotion of alveolar hyperplasia.

The size distribution of TiO_2 particle aggregate is shown in Figure 1D. Of 452 particle aggregates examined, 362 (80.1%) were nanosize, i.e. <100 nm. Overall, the average size was 84.9 nm and the median size was 44.4 nm.

IPS 9 day study—analysis of TiO_2

Female SD rats were treated with TiO_2 by IPS over a 9 day period (Figure 2A). Microscopic observation showed scattered inflammatory lesions with infiltration of numerous macrophages mixed with a few neutrophils and lymphocytes in TiO_2-treated animals. Overall, the number of macrophages in the alveoli was significantly increased in the TiO_2-treated animals (Figure 2B). As expected from the results of the IPS-initiation–promotion study, alveolar proliferative lesions were not observed (Figure 2C).

Morphologically, TiO_2 particles were observed as yellowish, polygonal bodies in the cytoplasm of cells (Figure 2D). These cells are morphologically distinct from neutrophils and strongly positive for CD68 (Figure 2E), indicating that the TiO_2 engulfing cells were macrophages. TiO_2 aggregates of various sizes were found in macrophages, and aggregates larger than a single macrophage were surrounded by multiple macrophages (supplementary Figure 1B is available at *Carcinogenesis* Online)

TEM also showed electron dense bodies in the cytoplasm of macrophages (Figure 2F and G). These bodies were found exclusively in macrophages and not found in the alveolar parenchyma, including alveolar epithelium and alveolar wall cells, or in any other cell type. The shape of the electron dense TiO_2 particles in the cytoplasm was quite similar to that observed in preparations taken from TiO_2 suspensions before administration (Figure 2H and supplementary Figure 1C and D is available at *Carcinogenesis* Online). Individual TiO_2 particles were rod-like in shape (supplementary Figure 1C is available at *Carcinogenesis* Online).

Element analysis by TEM and X-ray microanalysis indicated that these electron dense bodies were composed primarily of titanium particles (supplementary Figure 1E and F-1 and 1F-2 is available at *Carcinogenesis* Online). Titanium was not observed in the surrounding alveolar cells without electron dense bodies (supplementary Figure 1F-3 is available at *Carcinogenesis* Online). The size distribution of TiO_2 particle aggregates is shown in Figure 2I. Of 2571 particle aggregates examined, 1970 (76.6%) were <100 nm and five particles were >4000 nm in size. Overall, the average size was 107.4 nm and the median size was 48.1 nm.

IPS 9 day study—analysis of oxidative stress and inflammation-related factors in the lungs of wild-type rats

IPS of TiO_2 particles significantly increased SOD activity (Figure 3A) and 8-OHdG levels (Figure 3B) in the lungs of wild-type rats, but not in the mammary glands. Analysis of the expression levels of 12 cytokines using suspension array indicated that administration of TiO_2 particles significantly upregulated the expression of MIP1α, GRO and IL-6 in the lung tissue of wild-type rats (supplementary Table 2 is available at *Carcinogenesis* Online). MIP1α levels were slightly elevated (0.4 pg/mg protein) in the mammary gland (Figure 3C), although the elevation was not statistically significant. Elevation of MIP1α in the lung tissue of animals treated with TiO_2 particles was confirmed by western blotting (Figure 3D).

Immunohistochemically, MIP1α was detected in the cytoplasm of alveolar macrophages with phagocytosed TiO_2 particles (Figure 3E upper, stained in red) and these macrophages could be found in hyperplastic lesions of the lung (supplementary Figure 2A and B is available at *Carcinogenesis* Online). MIP1α was not detected in macrophages without TiO_2 particles (Figure 3E lower). Expression of CCR1, the major receptor of MIP1α, was observed in the lung; IPS of TiO_2 particles had little or no effect on CCR1 expression (supplementary Figure 2C is available at *Carcinogenesis* Online).

Effect of MIP1α on proliferation of a human lung cancer cell line in vitro

Alveolar macrophages were isolated from the lungs of SD rats and were confirmed to be macrophages by morphology and CD68 staining

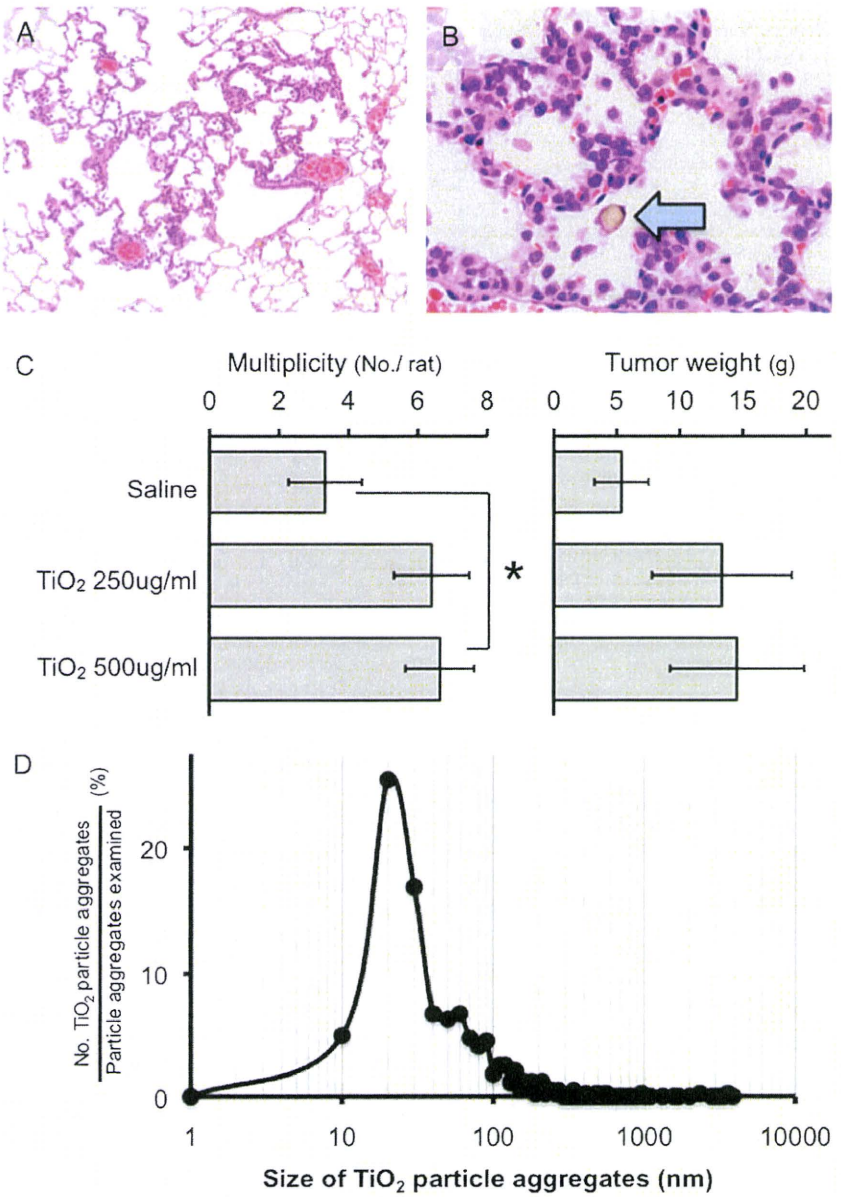

Fig. 1. Promoting effects of TiO_2 particles in DHPN-induced lung and mammary carcinogenesis (**A**) Alveolar hyperplasias observed in the lung of an H*ras*128 rat receiving DHPN and 500 μg/ml TiO_2 particles. (**B**) Alveolar macrophages with TiO_2 particles were also observed in hyperplasia lesions. (**C**) IPS of TiO_2 particles significantly increased the multiplicity of adenocarcinomas in the mammary gland and tended to increase the size of mammary tumors. (**D**) The size distribution of TiO_2 particle aggregates; among 452 particle aggregates examined, 362 (80.1%) were nanosize, i.e. <100 nm in diameter.

(data not shown). The macrophages were treated with TiO_2 particles suspended in saline (Figure 4A). TiO_2 induced secretion of MIP1α into the culture media (Figure 4B), and the culture medium collected from macrophages treated with TiO_2 particles promoted proliferation of A549 cells, whereas culture media collected from unexposed macrophages did not (Figure 4C). MIP1α neutralizing antibodies attenuated the promotion of A549 proliferation in a dose-dependent manner (Figure 4C). MIP1α-induced cell proliferation was also significantly suppressed by the ERK inhibitor PD98059 (Figure 4D). In addition, MIP1α increased ERK phosphorylation and PD98059 diminished ERK phosphorylation (Figure 4E).

We also examined the effect of MIP1α, GRO and IL-6, H_2O_2 and TiO_2 on the proliferation of A549 cells. MIP1α increased cell proliferation in a dose-dependent fashion, but GRO and IL-6 did not (supplementary Figure 3A–C is available at *Carcinogenesis* Online). H_2O_2 significantly suppressed cell proliferation, and antioxidant treatment diminished this suppression. Antioxidant treatment did not affect MIP1α-induced cell proliferation (supplementary Figure 3D is available at *Carcinogenesis* Online). These results suggest that ROS have no effect on tumor cell growth in this experiment.

In addition, TiO_2 did not directly increase proliferation of A549 cell (supplementary Figure 3E is available at *Carcinogenesis* Online).

Mechanism analysis of the promotion of mammary carcinogenesis

MIP1α was markedly elevated in the serum of the H*ras*128 rats treated with TiO_2 particles (Figure 5A). Serum levels of IL-6 were not changed by TiO_2 treatment and GRO was not detected in the serum

Table I. Effect of TiO2 on incidence and multiplicity of DHPN-induced alveolar hyperplasia and adenoma of the lung

Treatment	No. of rats	Alveolar hyperplasia		Lung adenoma	
		Incidence (%)	Multiplicity ## (no./cm^2)	Incidence (%)	Multiplicity # (no./cm^2)
Saline	9	9 (100)	5.91 ± 1.19	0	0
nTiO_2 250 mg/ml	10	10 (100)	7.36 ± 0.97*	1 (10)	0.10 ± 0.10
nTiO_2 500 mg/ml	11	11 (100)	11.05 ± 0.87**	4 (36)	0.46 ± 0.21*

*$P < 0.05$, **$P < 0.001$ versus saline control.
#$P < 0.05$, ##$P < 0.001$ in trend test (Spearman's rank correlation test).

(Figure 5A). MIP1α was slightly elevated in the mammary glands of these animals (Figure 5B); possibly, the elevated MIP1α detected in the mammary tissue was due to contamination by MIP1α in the serum. Recombinant MIP1α promoted the proliferation of C3 cells in a dose-dependent manner; a slight induction could be seen at a dose of 400 pg/ml and became statistically significant at the dose of 50 ng/ml (Figure 5C). Expression of CCR1, the major receptor of MIP1α, was observed in mammary tissue, and as in the lung, IPS of TiO_2 particles had little or no effect on CCR1 expression (data not shown). TiO_2 did not directly increase proliferation of C3 cells (supplementary Figure 3F is available at *Carcinogenesis* Online).

Discussion

To elucidate the mechanism underlying rat lung carcinogenesis by TiO_2 inhalation, we chose IPS. Although this method may be less physiological than the aerosol inhalation system, we observed that agglomerates and aggregates of TiO_2 particles from nano to micro size (mean diameter 107.4 nm) were diffusely distributed throughout the lung including peripheral alveoli, and they did not cause obstruction of the terminal bronchioles. Accordingly, IPS of TiO_2 particles can be expected to act similarly to aerosol inhalation of TiO_2.

Occupational exposure limits for TiO_2 in 13 countries or regions are 5–20 mg/m^3 (20), which results in TiO_2 exposure limits of 0.27–1.07 mg/kg body wt/day; calculations based on the human respiratory volume. In the present study, a total of 1.75 mg was administered per rat for 12 weeks in the high-dose group, resulting in a dose of 0.104 mg/kg body wt/day. Therefore, the dose we used in the present study was lower than the occupational exposure limit.

TiO_2, nanoscale and larger sized is evaluated as a Group 2B carcinogen by World Health Organization/International Agency for Research on Cancer (4) based on 2 year animal aerosol inhalation studies (3). We conducted the present carcinogenesis study using a two-step initiation–promotion protocol as a surrogate for a 2 year long-term protocol. Our study demonstrated that TiO_2 particles increased the multiplicity of alveolar cell hyperplasia and adenoma in the two-step IPS-initiation–promotion protocol. We used these lesions as endpoints in carcinogenicity testing because chemically induced tumors appear to be derived from hyperplasic lesions that progress to adenoma and carcinoma (21).

Several bioassay protocols based on the two-step carcinogenesis theory have been developed as practical and sensitive assays, and the compounds that exhibit promotion activity are considered to be carcinogens (22–29). Thus, our experimental design may be a practical surrogate for the long-term lung carcinogenesis protocol.

It should be noted that proliferative lesions including alveolar cell hyperplasia and adenomas were not found in the groups subjected to TiO_2 particle administration without prior treatment of DHPN. This is due to the weak carcinogenic potential and short duration of exposure to TiO_2 particles. Using the two-step IPS-initiation–promotion protocol, however, we did observe carcinogenic activity by this weak carcinogen. Thus, the two-step IPS-initiation–promotion protocol is an appropriate system to study carcinogenesis of TiO_2 particles and approximates long-term TiO_2 inhalation studies (3,11).

We next conducted a mechanism analysis of TiO_2 particle carcinogenesis focusing on the initial events induced by exposure to TiO_2 particles. Treatment with TiO_2 resulted in a modest infiltration of inflammatory cells into the alveolar space and septal wall, but the primary effect was a marked increase in the number of macrophages in the alveoli, and many of these macrophages contained phagocytosed TiO_2 particles. Alveolar macrophages play an important role in deposition and clearance of mineral fibers/particles, and macrophage activity is known to be strongly associated with inflammatory reactions and carcinogenesis caused by fibers and particles in the lung, including asbestos (30–33). ROS are known to be produced by macrophages upon particle phagocytosis (34,35). Clinical and experimental studies indicate that ROS production and resultant oxidative stress play an important role in cellular and tissue damage, inflammation and fibrosis in the lung. In our study, a significant increase in the activity of SOD and 8-OHdG formation in the lung were observed, indicating increased ROS production and DNA damage. Because macrophages are unable to detoxify TiO_2 particles, the reaction against these particles would be continuous over an extended period of time. This condition is associated with high levels of ROS production (36) and tissue toxicity (37).

Cytokine analysis of the lung tissue indicated that among the 12 cytokines examined, expression of IL-6, GRO and MIP1α were significantly higher in the TiO_2-treated group than in the vehicle group (supplementary Table 1 is available at *Carcinogenesis* Online). IL-6 is a pro-inflammatory cytokine that is involved in host defense as well as cancer development (38,39). IL-6 has been shown to be increased in lung tumor tissue (40,41) and in the sera of lung cancer patients (42). GRO, a member of the CXC chemokine family, has been shown to be involved in inflammatory responses, chemoattraction (43), carcinogenesis (44,45) and tumor progression (46). Thus, IL-6 and GRO may be involved in the promotion of lung carcinogenesis by TiO_2 (47).

Of the three cytokines induced by exposure to TiO_2 particles, however, we were particularly interested in MIP1α. This cytokine was not only induced in the lung tissue of TiO_2-treated rats, but, unlike IL-6 and GRO, it was also found in the serum of these animals. MIP1α is a member of the CC chemokine family and is primarily associated with cell adhesion and migration (17), proliferation and survival of myeloma cells (48). It is produced by macrophages in response to a variety of mineral particle-induced inflammatory stimuli (18). Our results indicate that expression of MIP1α by alveolar macrophages enhances the proliferation of A549 cells. Expression of CCR1, the major receptor of MIP1α, was observed in the lung tissue, rendering lung cells receptive to MIP1α induction of proliferation. Lung damage and inflammation induced by TiO_2 particles has also been reported to be associated with increased cell proliferation of lung epithelium cells (49), which is consistent with our results.

The MEK1–ERK-signaling pathway has been shown to be involved in CCR1 signaling (48). In the present study, the MEK1-specific inhibitor PD98059 suppressed MIP1α-induced cell proliferation and ERK phosphorylation. These results suggest that MEK1 is one of the downstream signaling molecules of MIP1α and the MEK1–ERK-signaling pathway may be partially involved in MIP1α signaling.

It should be noted that, in our IPS-initiation–promotion protocol, TiO_2 exposure also promoted DHPN-initiated mammary carcinogenesis. Our results suggest that MIP1α secreted by alveolar macrophages and transported via the circulatory system caused

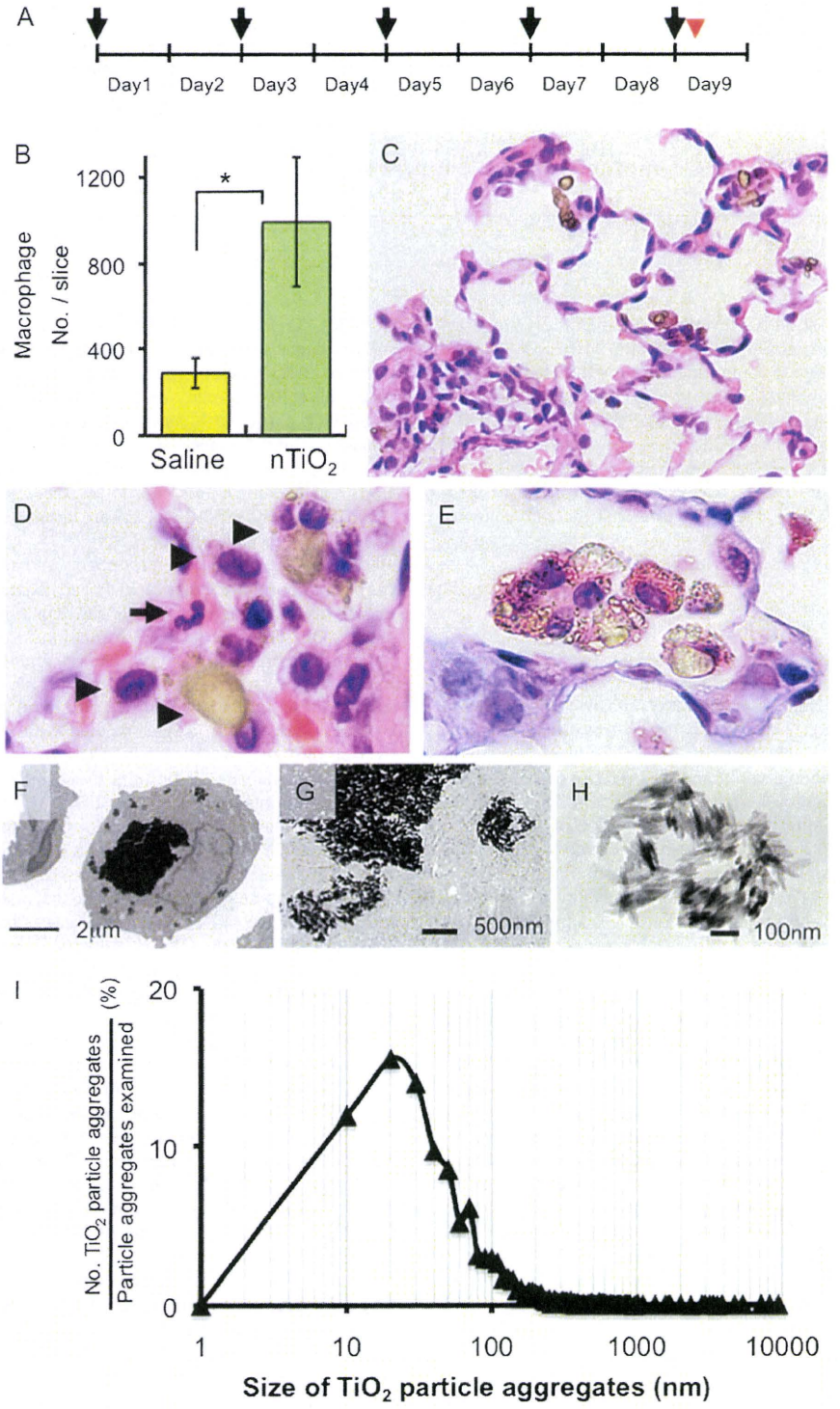

Fig. 2. TiO_2 particles in alveolar macrophages by light and electron microscopy (**A**) Twenty female SD rats (wild-type counterpart of H*ras*128) aged 10 weeks were treated by IPS with 0.5 ml suspension of 500 μg/ml TiO_2 particles in saline five times over a 9 day period. Arrows and arrowhead indicates IPS treatment and killing of the animals, respectively. (**B**) IPS of TiO_2 particles significantly increased the number of macrophages in the alveoli. (**C**) Inflammatory reactions were observed in the lung with slight infiltration of macrophages, neutrophils and lymphocytes. (**D**) TiO_2 particles were observed in alveolar macrophages (hematoxylin and eosin staining). Arrowheads indicate macrophages and the smaller cell indicated by the arrow is a neutrophil with its characteristic multilobular nucleus. (**E**) The multinucleated cells containing these particles were positive for the macrophage marker CD68 (Alkaline phosphatase reaction, red color). (**F**) TEM findings showed that TiO_2 particles of various sizes (~50 nm to 5 μm) were observed phagocytosed by alveolar macrophages. (**G**) Electron dense bodies were aggregates of TiO_2 particles. (**H**) TEM findings of TiO_2 particles in saline suspension before IPS. The shape of the TiO_2 particle aggregates was similar to those observed in macrophages. (**I**) The size distribution of TiO_2 particle aggregates: of 2571 particle aggregates examined, 1970 (77.1%) were <100 nm. The average size was 107.4 nm and the median size was 48.1 nm.

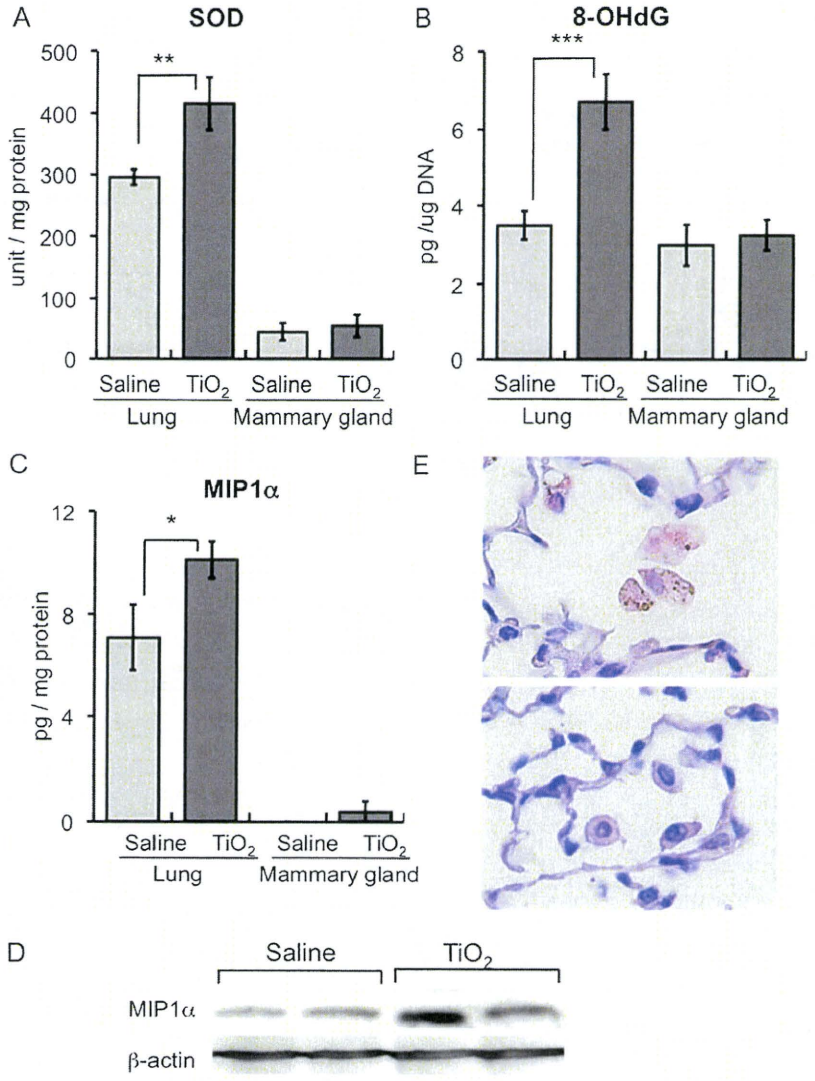

Fig. 3. Inflammatory factors upregulated in the lungs of wild-type rats by IT-spraying of TiO_2 particles in the IPS 9 day study (**A**) SOD activity and (**B**) 8-OHdG level in wild-type rats treated with TiO_2 particles or saline. (**C**) MIP1α protein level was significantly increased (142%) in the lung tissue of wild-type rats treated with TiO_2 (suspension array analysis). MIP1α was detected in the mammary gland of the TiO_2 group but not in the vehicle group. (**D**) In western blotting, expression of MIP1α was increased in the TiO_2 group compared with vehicle group. (**E**) MIP1α was immunohistochemically detected in alveolar macrophages containing TiO_2 particles (upper) but was not detected in macrophages of rats that were not exposed to TiO_2 particles (lower).

proliferation of mammary epithelial cells and thereby promoted mammary carcinogenesis. As with the lung, CCR1 was expressed by mammary cells, rendering these cells receptive to MIP1α induction of proliferation. While MIP1α secreted by alveolar macrophages would be diluted by the blood volume and while these levels may not be high enough to increase mammary cell proliferation in a short *in vitro* proliferation assay, it is possible that continuous low level stimulation over the course of 12 weeks could increase mammary cell proliferation in the environment of the mammary gland *in vivo*. Another possibility is that TiO_2 particles may act directly on the mammary gland after translocation to the mammary gland from the lung. However, TiO_2 exposure of mammary carcinoma cells did not induce proliferation *in vitro*. It must be understood that promotion of DHPN-induced mammary carcinogenesis by TiO_2 particles was observed in H*ras*128 female rats, and these animals are very highly susceptible to mammary carcinogenesis (50). Although, the effects we observed on promotion of mammary carcinogenesis in these animals may not be directly relevant to most humans, people at high risk for mammary carcinogenesis, such as individuals harboring BRCA mutations, may be a relevant population as regards the risk presented by nanoscale TiO_2.

Although our observations are based on results obtained with a mixed population of nanoscale and larger sized particle aggregates, size analysis indicated that 80.1% of them were nanoscale (<100 nm in diameter) in the 16 week IPS-initiation–promotion study and 76.6% were nanoscale in the IPS 9 day study. Thus, the results can be interpreted as being strongly associated with nanoscale particle aggregates.

In conclusion, the IPS-initiation–promotion protocol detected TiO_2 carcinogenic activity in the rat lung and is therefore comparable, at least for TiO_2 inhalation, to a long-term whole body inhalation carcinogenesis study. We also elucidated a plausible mechanism for the carcinogenic effect of TiO_2 particles in the rat lung. Phagocytosis of TiO_2 particles by alveolar macrophages resulted in ROS production and DNA damage and increased expression of MIP1α. MIP1α in turn was able to enhance proliferation of lung epithelium cells. Thus, lung

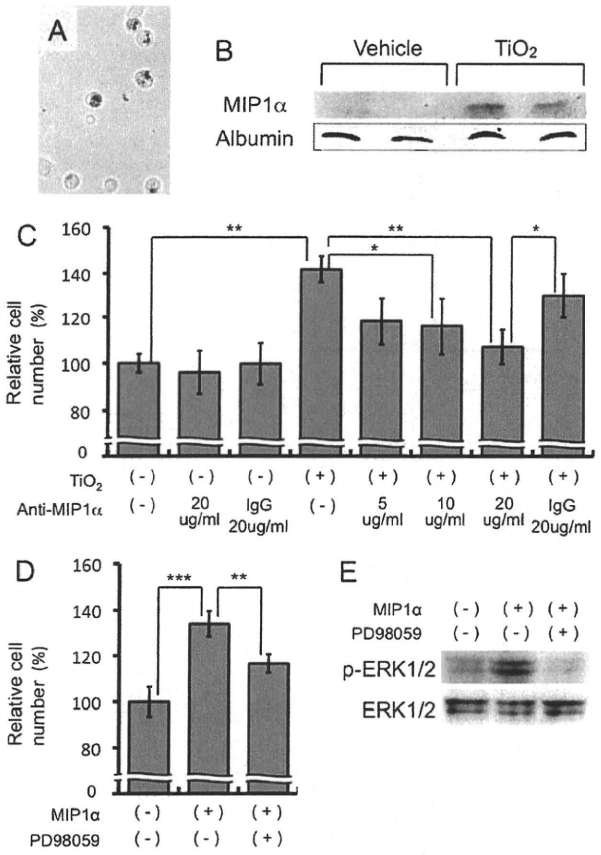

Fig. 4. Growth stimulation effects of conditioned medium from alveolar macrophages on human lung cancer cell lines. (**A**) Primary cultured alveolar macrophages of rats were treated with TiO_2 particles. (**B**) MIP1α was detected in the culture medium. (**C**) The number of A549 cells was significantly increased by addition of conditioned medium from alveolar macrophages treated with TiO_2 particles. MIP1α neutralizing antibody attenuated this effect in a dose-dependent manner. Irrelevant IgG was used as control antibody. (**D**) MIP1α-induced cell proliferation was significantly suppressed by the ERK inhibitor PD98059. (**E**) MIP1α increased ERK phosphorylation and PD98059 diminished this phosphorylation.

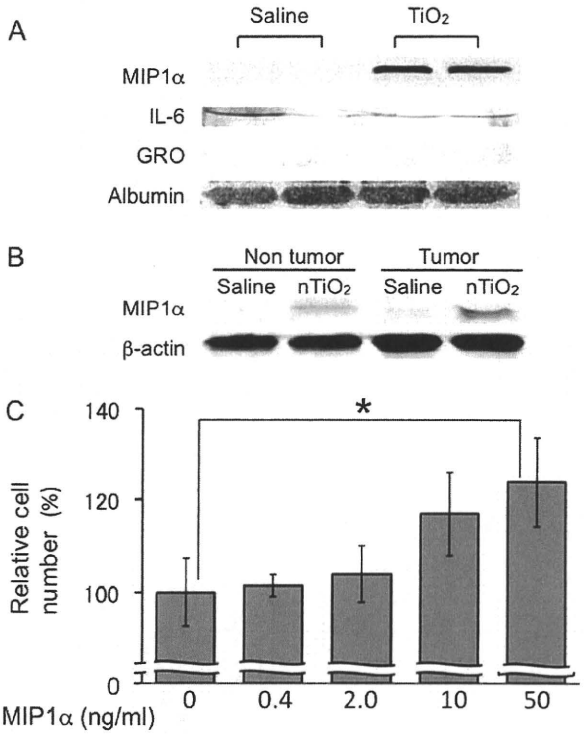

Fig. 5. Promotion effects of MIP1α on proliferation of a rat mammary cancer cell line, C3 (**A**) MIP1α was detected in the serum of the H*ras*128 rats treated with TiO_2 but not in vehicle control rats in the 16 week study. No difference in IL-6 in the serum was observed and GRO was not detected in the serum. (**B**) MIP1α levels are slightly elevated in non-tumor and tumor tissue of the mammary gland of animals treated by IPS with TiO_2 particles in the 16 week study. (**C**) Recombinant MIP1α increased the number of rat mammary carcinoma C3 cells in a dose-dependent manner ($P = 0.0127$).

tissue exposed to TiO_2 particles exhibits increase in both DNA damage and proliferation. Importantly, a similar mechanism would function in humans in the promotion of lung carcinogenesis associated with inhalation of TiO_2 particles and other nanoparticles with the capacity to form aggregates. In addition, TiO_2 administered to the lung had carcinogenic activity in the H*ras*128 transgenic rat mammary gland; this carcinogenic activity is probably mediated via serum MIP1α resulting from expression of MIP1α by alveolar macrophages. This finding may indicate that exposure of TiO_2 particles is a risk factor for mammary carcinogenesis in predisposed populations, such as individuals with BRCA mutations.

Supplementary material

Supplementary Figures 1–3 and Tables 1 and 2 can be found at http://carcin.oxfordjournals.org/

Funding

Health and Labour Sciences Research Grants, Ministry of Health, Labour and Welfare, Japan (Research on Risk of Chemical Substance 21340601, H18-kagaku-ippan-007); a grant-in-aid for the Second Term Comprehensive 10 Year Strategy for Cancer Control, Ministry of Health, Labour and Welfare, Japan; grants-aid for Cancer Research, Ministry of Education, Culture, Sports, Science and Technology.

Acknowledgements

Conflict of Interest Statement: None declared.

References

1. Oberdorster,G. (2002) Toxicokinetics and effects of fibrous and nonfibrous particles. *Inhal. Toxicol.*, **14**, 29–56.
2. Romundstad,P. *et al.* (2001) Cancer incidence among workers in the Norwegian silicon carbide industry. *Am. J. Epidemiol.*, **153**, 978–986.
3. Pott,F. *et al.* (2005) Carcinogenicity study with nineteen granular dusts in rats. *Eur. J. Oncol.*, **10**, 249–281.
4. Baan,R. *et al.* (2006) Carcinogenicity of carbon black, titanium dioxide, and talc. *Lancet Oncol.*, **7**, 295–296.
5. Schulte,P. *et al.* (2008) Occupational risk management of engineered nanoparticles. *J. Occup. Environ. Hyg.*, **5**, 239–249.
6. Maynard,A.D. *et al.* (2006) Safe handling of nanotechnology. *Nature*, **444**, 267–269.
7. Scheringer,M. (2008) Nanoecotoxicology: environmental risks of nanomaterials. *Nat. Nanotechnol.*, **3**, 322–323.
8. Borm,P. *et al.* (2006) Research strategies for safety evaluation of nanomaterials, part V: role of dissolution in biological fate and effects of nanoscale particles. *Toxicol. Sci.*, **90**, 23–32.
9. Phalen,R.F. (1976) Inhalation exposure of animals. *Environ. Health Perspect.*, **16**, 17–24.

10. Mauderly,J.L. (1997) Relevance of particle-induced rat lung tumors for assessing lung carcinogenic hazard and human lung cancer risk. *Environ. Health Perspect.*, **105** (suppl. 5), 1337–1346.
11. Roller,M. *et al.* (2006) Lung tumor risk estimates from rat studies with not specifically toxic granular dusts. *Ann. N. Y. Acad. Sci.*, **1076**, 266–280.
12. Imaida,K. *et al.* (1996) Initiation-promotion model for assessment of carcinogenicity: medium-term liver bioassay in rats for rapid detection of carcinogenic agents. *J. Toxicol. Sci.*, **21**, 483–487.
13. IARC (1999) The use of short-and medium-term tests for carcinogens and data on genetic effects in carcinogenic hazard evaluation. Consensus report. *IARC Sci. Publ.*, **146**, 1–18.
14. Asamoto,M. *et al.* (2000) Transgenic rats carrying human c-Ha-ras proto-oncogenes are highly susceptible to N-methyl-N-nitrosourea mammary carcinogenesis. *Carcinogenesis*, **21**, 243–249.
15. Han,B.S. *et al.* (2002) Inhibitory effects of 17beta-estradiol and 4-n-octylphenol on 7,12-dimethylbenz[a]anthracene-induced mammary tumor development in human c-Ha-ras proto-oncogene transgenic rats. *Carcinogenesis*, **23**, 1209–1215.
16. Ohnishi,T. *et al.* (2007) Possible application of human c-Ha-ras proto-oncogene transgenic rats in a medium-term bioassay model for carcinogens. *Toxicol. Pathol.*, **35**, 436–443.
17. Terpos,E. *et al.* (2005) Significance of macrophage inflammatory protein-1 alpha (MIP-1alpha) in multiple myeloma. *Leuk. Lymphoma*, **46**, 1699–1707.
18. Driscoll,K.E. *et al.* (1993) Macrophage inflammatory proteins 1 and 2: expression by rat alveolar macrophages, fibroblasts, and epithelial cells and in rat lung after mineral dust exposure. *Am. J. Respir. Cell Mol. Biol.*, **8**, 311–318.
19. Hamaguchi,T. *et al.* (2006) Establishment of an apoptosis-sensitive rat mammary carcinoma cell line with a mutation in the DNA-binding region of p53. *Cancer Lett.*, **232**, 279–288.
20. IARC (1989) Titanium dioxide. *IARC monograph Evaluation of carcinogenic risks to humans*. IARC Scientific Publications, Lyon, vol. 47, pp. 307–326.
21. Stoner,G.D. *et al.* (1993) Lung tumors in strain A mice: application for studies in cancer chemoprevention. *J. Cell. Biochem. Suppl.*, **17F**, 95–103.
22. Pitot,H.C. *et al.* (1978) Biochemical characterisation of stages of hepatocarcinogenesis after a single dose of diethylnitrosamine. *Nature*, **271**, 456–458.
23. Peraino,C. *et al.* (1971) Reduction and enhancement by phenobarbital of hepatocarcinogenesis induced in the rat by 2-acetylaminofluorene. *Cancer Res.*, **31**, 1506–1512.
24. Ito,N. *et al.* (2003) A medium-term rat liver bioassay for rapid *in vivo* detection of carcinogenic potential of chemicals. *Cancer Sci.*, **94**, 3–8.
25. Ito,N. *et al.* (1988) Wide-spectrum initiation models: possible applications to medium-term multiple organ bioassays for carcinogenesis modifiers. *Jpn. J. Cancer Res.*, **79**, 413–417.
26. IARC (1980) Long-term and short-term screening assays for carcinogens: a critical appraisal. *IARC Scientific Publications, Lyon, vol.* 83 (suppl. 2), pp. 1–146.
27. Konishi,Y. *et al.* (1987) Lung carcinogenesis by N-nitrosobis(2-hydroxypropyl)amine-related compounds and their formation in rats. *IARC Sci. Publ.*, **82**, 250–252.
28. Nishikawa,A. *et al.* (1994) Effects of cigarette smoke on N-nitrosobis(2-oxopropyl)amine-induced pancreatic and respiratory tumorigenesis in hamsters. *Jpn. J. Cancer Res.*, **85**, 1000–1004.
29. Yamanaka,K. *et al.* (1996) Exposure to dimethylarsinic acid, a main metabolite of inorganic arsenics, strongly promotes tumorigenesis initiated by 4-nitroquinoline 1-oxide in the lungs of mice. *Carcinogenesis*, **17**, 767–770.
30. Rom,W.N. *et al.* (1991) Cellular and molecular basis of the asbestos-related diseases. *Am. Rev. Respir. Dis.*, **143**, 408–422.
31. Heppleston,A.G. (1984) Pulmonary toxicology of silica, coal and asbestos. *Environ. Health Perspect.*, **55**, 111–127.
32. Renwick,L.C. *et al.* (2001) Impairment of alveolar macrophage phagocytosis by ultrafine particles. *Toxicol. Appl. Pharmacol.*, **172**, 119–127.
33. Rimal,B. *et al.* (2005) Basic pathogenetic mechanisms in silicosis: current understanding. *Curr. Opin. Pulm. Med.*, **11**, 169–173.
34. Wang,Y. *et al.* (2007) The role of the NADPH oxidase complex, p38 MAPK, and Akt in regulating human monocyte/macrophage survival. *Am. J. Respir. Cell Mol. Biol.*, **36**, 68–77.
35. Bhatt,N.Y. *et al.* (2002) Macrophage-colony-stimulating factor-induced activation of extracellular-regulated kinase involves phosphatidylinositol 3-kinase and reactive oxygen species in human monocytes. *J. Immunol.*, **169**, 6427–6434.
36. Dorger,M. *et al.* (2000) Comparison of the phagocytic response of rat and hamster alveolar macrophages to man-made vitreous fibers *in vitro*. *Hum. Exp. Toxicol.*, **19**, 635–640.
37. Blake,T. *et al.* (1998) Effect of fiber length on glass microfiber cytotoxicity. *J. Toxicol. Environ. Health A*, **54**, 243–259.
38. Kabir,S. *et al.* (1995) Serum levels of interleukin-1, interleukin-6 and tumour necrosis factor-alpha in patients with gastric carcinoma. *Cancer Lett.*, **95**, 207–212.
39. Schneider,M.R. *et al.* (2000) Interleukin-6 stimulates clonogenic growth of primary and metastatic human colon carcinoma cells. *Cancer Lett.*, **151**, 31–38.
40. Asselin-Paturel,C. *et al.* (1998) Quantitative analysis of Th1, Th2 and TGF-beta1 cytokine expression in tumor, TIL and PBL of non-small cell lung cancer patients. *Int. J. Cancer*, **77**, 7–12.
41. Matanic,D. *et al.* (2003) Cytokines in patients with lung cancer. *Scand. J. Immunol.*, **57**, 173–178.
42. Brichory,F.M. *et al.* (2001) An immune response manifested by the common occurrence of annexins I and II autoantibodies and high circulating levels of IL-6 in lung cancer. *Proc. Natl Acad. Sci. USA*, **98**, 9824–9829.
43. Rollins,B.J. (1997) Chemokines. *Blood*, **90**, 909–928.
44. Zhou,Y. *et al.* (2005) The chemokine GRO-alpha (CXCL1) confers increased tumorigenicity to glioma cells. *Carcinogenesis*, **26**, 2058–2068.
45. Yang,G. *et al.* (2006) The chemokine growth-regulated oncogene 1 (Gro-1) links RAS signaling to the senescence of stromal fibroblasts and ovarian tumorigenesis. *Proc. Natl Acad. Sci. USA*, **103**, 16472–16477.
46. Li,A. *et al.* (2004) Constitutive expression of growth regulated oncogene (gro) in human colon carcinoma cells with different metastatic potential and its role in regulating their metastatic phenotype. *Clin. Exp. Metastasis*, **21**, 571–579.
47. Rollins,B.J. (2006) Inflammatory chemokines in cancer growth and progression. *Eur. J. Cancer*, **42**, 760–767.
48. Lentzsch,S. *et al.* (2003) Macrophage inflammatory protein 1-alpha (MIP-1 alpha) triggers migration and signaling cascades mediating survival and proliferation in multiple myeloma (MM) cells. *Blood*, **101**, 3568–3573.
49. Baggs,R.B. *et al.* (1997) Regression of pulmonary lesions produced by inhaled titanium dioxide in rats. *Vet. Pathol.*, **34**, 592–597.
50. Tsuda,H. *et al.* (2001) High susceptibility of transgenic rats carrying the human c-Ha-ras proto-oncogene to chemically-induced mammary carcinogenesis. *Mutat. Res.*, **477**, 173–182.

Received September 27, 2009; revised January 14, 2010; accepted January 24, 2010

Journal of Environmental Science and Health Part A (2010) **45**, 1616–1624

ISSN: 1093-4529 (Print); 1532-4117 (Online)
DOI: 10.1080/10934529.2010.506121

Taylor & Francis
Taylor & Francis Group

Chloroform distribution and accumulation by combined inhalation plus oral exposure routes in rats

MAKOTO TAKE[1], SEIGO YAMAMOTO[1], MAKOTO OHNISHI[1], MICHIHARU MATSUMOTO[1], KASUKE NAGANO[1], TAKASHI HIROTA[2] and SHOJI FUKUSHIMA[1]

[1]*Japan Bioassay Research Center, Japan Industrial Safety and Health Association, Hadano, Kanagawa, Japan*
[2]*Department of Biopharmaceutics, Faculty of Pharmaceutical Sciences, Tokyo University of Science, Noda, Chiba, Japan*

The present investigation was undertaken to determine the distribution and accumulation of chloroform in the blood, liver, kidney and abdominal fat of rats after simultaneous exposure by two routes, inhalation and oral. To distinguish the contribution of each route, unmodified chloroform ($CHCl_3$) was administered by inhalation and deuterated chloroform ($CDCl_3$) was administered orally. Exposure by inhalation and oral administration resulted in $CHCl_3$ and $CDCl_3$ concentrations in the tissues which were significantly higher than when exposure was by either inhalation or oral administration alone. This is the first study to follow the contribution of each of two routes of chloroform exposure on chloroform distribution and accumulation in target tissues. Our results indicate that when assessing the toxicity and carcinogenicity of chloroform, exposure routes, especially the effects of exposure by multiple routes, must be taken into consideration.

Keywords: Chloroform, deuterated chloroform, combined exposure routes, blood concentration, tissue concentration, mass spectrometer.

Introduction

Chloroform is widely used as an organic solvent during the synthesis of fluorocarbons, drugs and insecticide fumigants,[1] and substantial amounts have been released into the atmosphere and public water supply.[2,3] Chloroform is also produced by sanitary chlorination of drinking water. Andelman[4] and the Ministry of the Environmental Government of Japan[5] have reported that chloroform is present in outdoor and indoor air, community drinking water, and a variety of foodstuffs. Consequently, humans are potentially exposed to chloroform through various media including the air and water.

Chloroform is categorized as a possible human carcinogen (2B) by the International Agency for Research on Cancer (IARC).[1] Animal studies have shown that both inhalation[6] and oral[7,8] administration of chloroform induces kidney tumors in rats and mice. Importantly, a two year study using rats indicated that compared with either inhalation or oral administration alone, combined inhalation plus oral administration of chloroform markedly enhanced chloroform toxicity and tumor induction in the kidney.[9] This study concluded that the enhanced effect on renal toxicity and carcinogenicity of exposure to chloroform by inhalation plus oral administration was greater than additive. That the effect of exposure to a chemical mixture by multiple routes may be different from the additive effects of exposure by single routes is also espoused by the United States Environmental Protection Agency (US EPA).[10]

The blood concentration of chloroform,[11–15] the distribution of chloroform into the blood and tissues[16,17] and a physiologically based pharmacokinetic model for chloroform[18] after exposure by a single route have been described by previous papers. However, because of the non-additive effect of multiple-route exposure to chloroform, it is also important to determine the contribution of each route of a multiple-route exposure to the concentration of chloroform in the blood and tissues. The aim of the present study was to use 2 routes of exposure to chloroform, administration by inhalation and administration by oral gavage, and determine the contribution of each exposure route to chloroform concentrations in the blood and tissues. In order to assess each exposure route, we administered unmodified chloroform ($CHCl_3$) by inhalation and deuterated chloroform ($CDCl_3$) via oral gavage and analyzed $CHCl_3$ and $CDCl_3$ by mass spectrometer (MS). The present study is the first report on these determinations.

Address correspondence to Makoto Take, Japan Bioassay Research Center, Japan Industrial Safety and Health Association, Kanagawa, Japan; E-mail: m-take@jisha.or.jp
Received March 25, 2010.

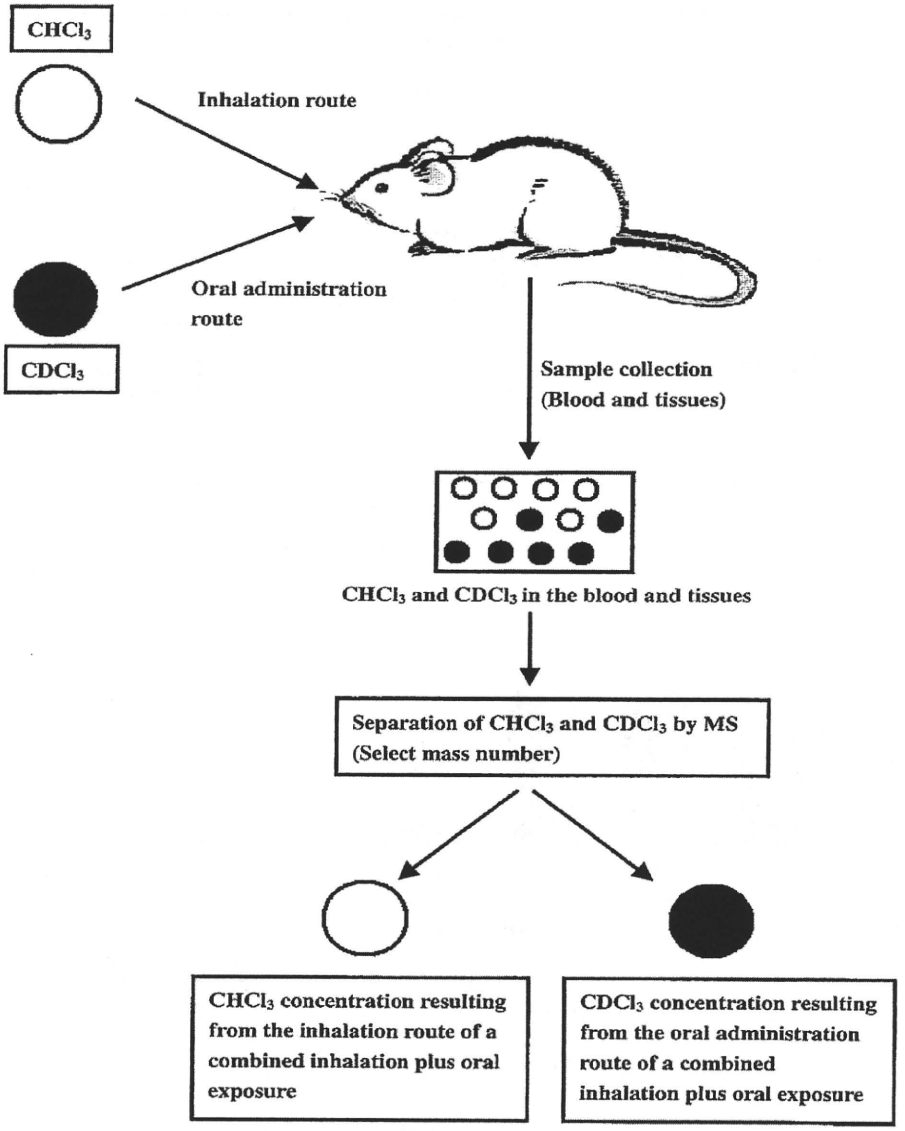

Fig. 1. Following the chloroform delivered by inhalation ($CHCl_3$) and the chloroform delivered orally ($CDCl_3$) when chloroform is administered simultaneously by inhalation and oral gavage.

Materials and methods

Chemicals

$CHCl_3$ (purity greater than 99.0%) used for inhalation administration was purchased from Wako Pure Chemical Industries, Ltd (Osaka, Japan) and $CDCl_3$ (purity greater than 98.0%) used for oral administration was purchased from Cambridge Isotope Laboratories, Inc (Andover, MA, USA).

Animal care

17-wk-old male F344/DuCrj SPF rats were purchased from Charles River Japan, Inc. (Kanagawa, Japan): body weights ranged from 243 to 301 g. Experiments were started after a one week acclimation period. The temperature and the relative humidity of the study were maintained in the ranges of 23 ± 2°C and 55 ± 15%, respectively. The animals were cared for according to the Guide for the Care and Use of Laboratory Animals,[19] and the present study was approved by the ethics committee of the Japan Bioassay Research Center (JBRC).

Study design

The rats were divided into 3 groups: inhalation administration, oral administration and combined inhalation plus oral administration. In the inhalation administration group, rats

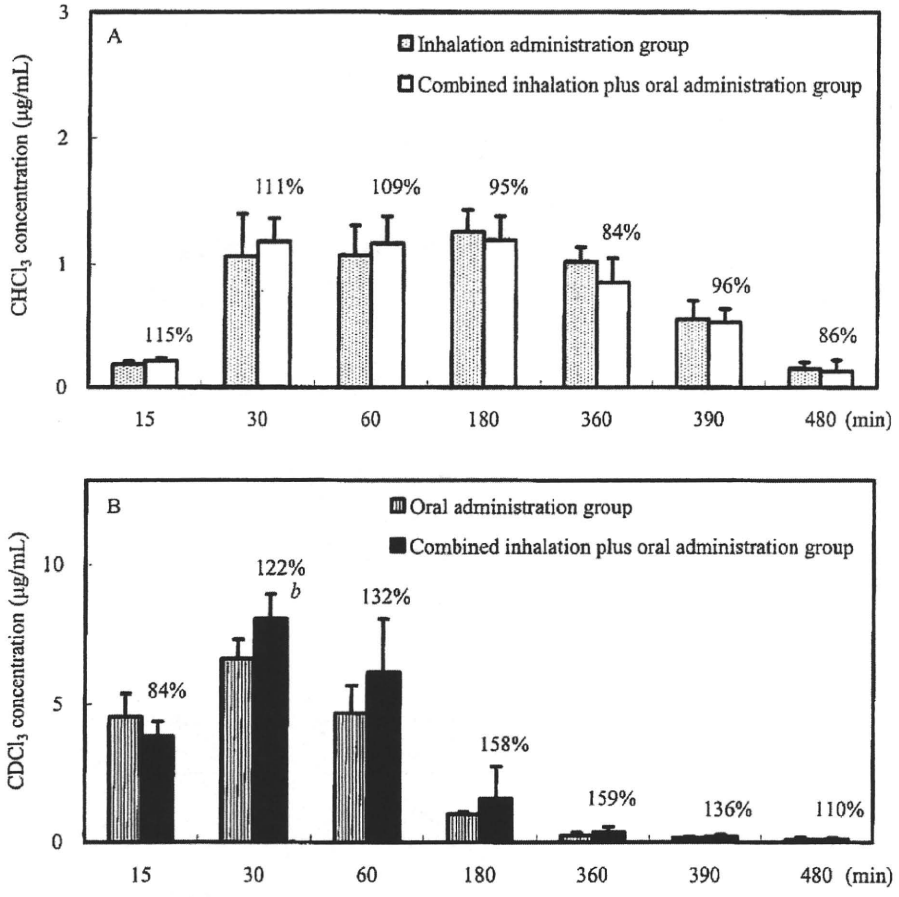

Fig. 2. $CHCl_3$ and $CDCl_3$ concentrations (mean ± SD) in the blood at each collection time point (n = 5 for each collection time/group): (A) Inhalation route. Numbers above the SD bars represent the percentage ratio of the $CHCl_3$ concentration in the blood of the combined inhalation plus oral administration group to the $CHCl_3$ concentration in the blood of the inhalation administration group at each collection time point. (B) Oral administration route. Numbers above the SD bars represent the percentage ratio of the $CDCl_3$ concentration in the blood of the combined inhalation plus oral administration group to the $CDCl_3$ concentration in the blood of the oral administration group at each collection time. ^{b}Significantly different from the oral administration group ($P \leq 0.05$).

were exposed to $CHCl_3$ by inhalation using whole-body inhalation chambers.[15] $CHCl_3$ vapor at a concentration of 100 ppm was generated by bubbling clean air through liquid $CHCl_3$. The $CHCl_3$ vapor concentration in the inhalation chambers was measured with gas chromatography (GC) using Agilent Technologies 6890 (Agilent Technologies, Santa Clara, CA, USA) every 15 min during the inhalation exposure period. The target concentration of $CHCl_3$ was 100 ppm (v/v) for 360 min. This dose is the same as one daily dose used by Nagano et al.[9] In the oral administration group, $CDCl_3$ dissolved in water (1000 ppm (w/w)) was orally administrated by stomach tube at a dose of 55 mg/kg body weight. This dose is equivalent to one daily dose of $CHCl_3$ administered at 1000 ppm $CHCl_3$ in the drinking water.[9] In the combined inhalation plus oral administration group, rats were exposed to $CHCl_3$ by inhalation at a target concentration of 100 ppm for 360 min immediately after the oral gavage of $CDCl_3$ at a dose of 55 mg/kg body weight (Fig. 1). The $CHCl_3$ vapor concentration in the inhalation chambers was 100.3 ± 0.99 and 100.4 ± 1.62 ppm (mean ± SD) in the inhalation administration and combined inhalation plus oral administration groups, respectively.

Blood and tissues collections and pretreatment for measurement

Forty-five rats in each group were used for examination of $CHCl_3$ and $CDCl_3$ concentrations in the blood and tissues. Blood was collected from the tail vein of each rat, and afterwards, necropsy was performed on the rats under ether anesthesia at 0, 15, 30, 60, 180, 360, 390, 480 or 1440 min after the start of inhalation administration or oral administration (5 rats were used for each collection time/group). The 0.2 mL blood samples were collected into 10-mL headspace sampler (HS)-vials and

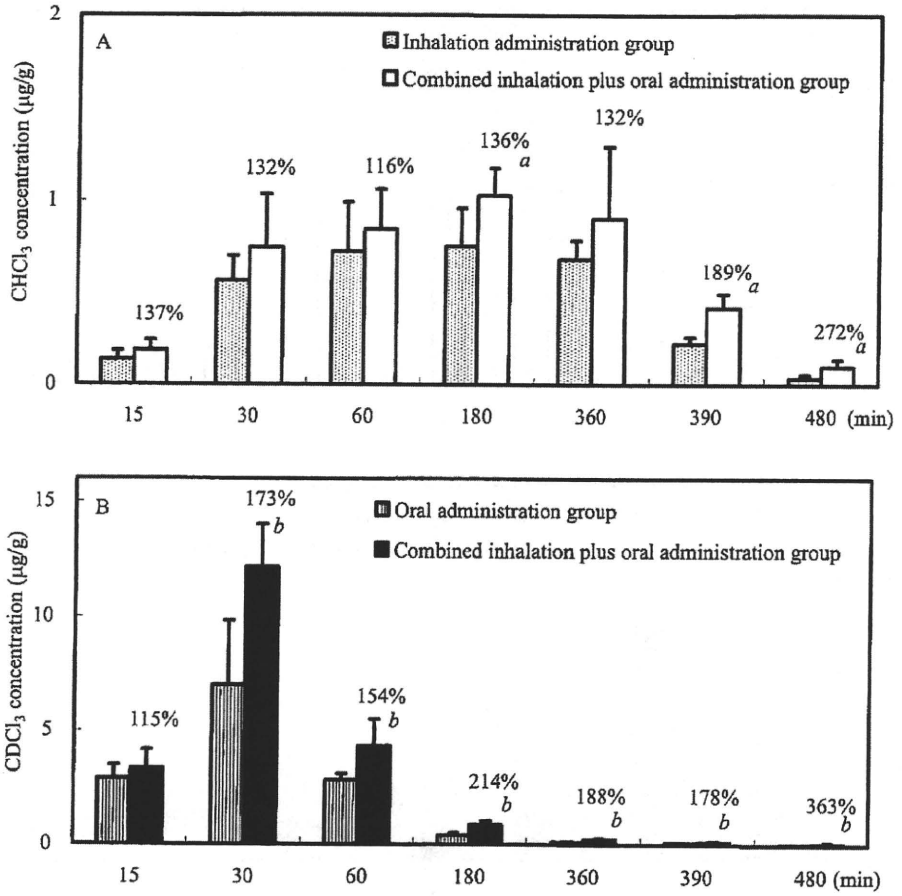

Fig. 3. $CHCl_3$ and $CDCl_3$ concentrations (mean ± SD) in the liver at each collection time point (n = 5 for each collection time/group): (A) Inhalation route. Numbers above the SD bars represent the percentage ratio of the $CHCl_3$ concentration in the liver of the combined inhalation plus oral administration group to the $CHCl_3$ concentration in the liver of the inhalation administration group at each collection time point. [a]Significantly different from the inhalation administration group ($P \leq 0.05$). (B) Oral administration route. Numbers above the SD bars represent the percentage ratio of the $CDCl_3$ concentration in the liver of the combined inhalation plus oral administration group to the $CDCl_3$ concentration in the liver of the oral administration group at each collection time. [b]Significantly different from the oral administration group ($P \leq 0.05$).

0.2 mL of distilled water was added to each sample. The liver, kidney and abdominal fat were removed from each rat and each tissue sample (liver, kidney and abdominal fat: range from about 0.1 to 1 g) was placed into a 10-mL HS-vial. 5 mL of distilled water was then added and the vials were immediately sealed with an aluminum crimp cup. $CHCl_3$ and $CDCl_3$ were not detected in the blood and tissues at time 0 or 1440 min (data not shown) in the 3 groups.

Measurement of $CHCl_3$ and $CDCl_3$ in the blood and tissues

The $CHCl_3$ and $CDCl_3$ concentrations in the blood and tissue samples were analyzed by HS-GC/MS using Agilent Technologies 7694 (Agilent Technologies) HS (oven temperature, 60°C; loop temperature, 80°C; vial equilibration time, 10 min (blood) and 30 min (tissues)) and Hitachi M-80B (Hitachi, Tokyo, Japan) GC/MS system (column, Agilent Technologies INNOWax 15 m × 0.53 mm i.d.; oven temperature, 80°C; ion source temperature, 250°C; carrier gas, helium at 10 mL/min; ionization, EI (electron ionization); collector slit, 150 μm; fragment peak, 82.946 m/z ($CHCl_3$) and 83.953 m/z ($CDCl_3$)).

Statistical analysis

Results are represented as means ± SD. Statistical comparison was performed between the single exposure route and the combined exposure routes using Student's *t*-test. A P value of 0.05 was considered significant.